RECUMBENT VS UPRIGHT BICYCLES: 3D TRAJECTORY OF BODY CENTRE OF MASS, LIMB MECHANICAL WORK, AND OPERATIVE RANGE OF PROPULSIVE MUSCLES.

Running title: Comparison between Recumbent and Upright Bicycles

Keywords: cycling, mechanical power, muscle length, centre of mass, recumbent.

Authors: RICCARDO TELLI[1], ELENA SEMINATI*[2,1], GASPARE PAVEI[1] &, ALBERTO ENRICO MINETTI[1]

[1]*Università degli Studi di Milano, Department of Pathophysiology and Transplantation, Division of Physiology, Via Mangiagalli 32, 20133, Milano, Italy.*

[2]*University of Bath, Department for Health, Claverton Down Road, Bath, North East Somerset, BA2 7AY, UK.*

***Corresponding author**:

Dr Elena Seminati, Sport, Health & Exercise Science, Department for Health | University of Bath, Applied Biomechanics Suite, 1.308, BA2 7AY, BATH (UK). Email: elenaseminati@yahoo.com or e.seminati@bath.ac.uk

E-mail of the other authors:

Riccardo Telli: riccardo.telli@libero.it

Gaspare Pavei: gaspare.pavei@unimi.it

Alberto Enrico Minetti: alberto.minetti@unimi.it

Acknowledgements: The authors would like to thank all the participants who took part to the experimental sessions. They also acknowledge the assistance provided by Dr Dario Cazzola and Dr Carlo Biancardi, who contributed to data collection and support for the whole experimental sessions and Dr Carly Mckay for the manuscript proofreading.

Abstract

Recumbent bicycles (RB) are high performance, human powered vehicles. In comparison to normal/upright bicycles (NB) the RB may allow individuals to reach higher speeds due to aerodynamic advantages. The purpose of this investigation was to compare the non-aerodynamic factors that may potentially influence the performance of the two bicycles. 3D Body Centre of Mass (BCoM) trajectory, its symmetries, and the components of the total mechanical work necessary to sustain cycling were assessed through 3D kinematics and computer simulations. Data collected at 50, 70, 90 110 rpm during stationary cycling were used to drive musculoskeletal modelling simulation and estimate muscle-tendon length. Results demonstrated that BCoM trajectory, confined in a 15 mm side cube, changed its orientation, maintaining a similar pattern across all cadences in both bicycles. RB displayed a reduced additional mechanical external power (16.1 ± 9.7 W on RB versus 20.3 ± 8.8 W on NB), a greater symmetry on the progression axis, and no differences in the internal mechanical power compared to NB. Simulated muscle activity revealed small significant differences for only selected muscles. On the RB, quadriceps and gluteus demonstrated greater shortening, while biceps femoris, iliacus and psoas exhibited greater stretch; however, aerodynamics still remains the principal benefit.

Introduction

Humans have always aimed to move safely and faster, even through the aid of passive tools that help to improve the limits imposed by body characteristics. These means of locomotion, without supplying additional mechanical energy, are able to greatly improve performance by exploiting the use of muscular force alone. The most commonly used passive tool in the world is the bicycle (Minetti, 2004). When pedalling, body weight is supported by the saddle and not by the limbs, allowing muscle power to be exploited mainly for propulsion rather than for posture maintenance.

Since the first bicycle was introduced in the 1820s, different models have been developed throughout the entire twentieth century. Muscle efficiency was optimized by using gears while rolling resistance and aerodynamic drag were reduced utilizing inflated tyres and by designing new vehicles (Minetti, Pinkerton, & Zamparo, 2001). In 1933 the Recumbent Bicycle (RB) was introduced, allowing higher speeds at the same metabolic power compared to the Normal/Upright Bicycle (NB) principally due to aerodynamic advantages (Gross, Kyle, & Malewicki, 1983). RB were never formally included in official competitions, however with the use of particular fairings, they became the fasted human powered vehicles, allowing speeds in excess of 130 km/h (from the International Human Powered Vehicle Association website: http://www.ihpva.org/hpvarec3.htm#nom01).

Changing the position of the subject on a bicycle alters both biomechanics and energetics of pedalling, and the effects of different posture have been investigated both in upright (Faria, Parker, & Faria, 2005) and recumbent cycling (Too, 1990). However, some relevant physiological and biomechanical parameters such the Body Centre of Mass (BCoM) trajectory and its associated symmetries have often been neglected and have never been experimentally calculated for the recumbent bicycle. Also, no study has

investigated the different components of the total mechanical work (W_{TOT}) and muscle-tendon length changes when cycling on this type of vehicle.

The total mechanical energy changes (the mechanical work) necessary to maintain overall motion influence metabolic energy expenditure in locomotion. The mechanical external work (W_{EXT}) necessary to raise and accelerate the BCoM in walking and running is referred to in cycling as the work necessary to overcome rolling and air resistance (Minetti et al., 2001). However, the common belief of a purely horizontal translational pattern of the BCoM in cycling was suggested not to be the case (Minetti, 2011). Rather, the small BCoM movements described an elliptical trajectory in the sagittal plane that could be responsible for the slight additional mechanical external work (W_{EXT*}) necessary to sustain the periodic lift and acceleration of the BCoM, even when pedalling seated on a saddle. The work necessary to reciprocally accelerate body segments with respect to the BCoM (Cavagna & Kaneko, 1977), but also including the work to overcome internal friction in body tissues (Fenn, 1930), is described by the mechanical internal work (W_{INT}). This component was investigated only on upright bicycles in terms of metabolic equivalent of internal power during pedalling ($\dot{W}_{INT}$) and it was modelled to depend on the third power of the pedalling frequency (di Prampero, Mognoni, & Saibene, 1979; Minetti et al., 2001).

Different cycling positions bring trunk and lower limbs in different configurations that could have consequences not only on the mechanical work, but also on the behaviour of the propulsive muscles. Maganaris estimated the force-length characteristics of the in *vivo* skeletal muscles during ankle movements. His results showed that the medial and lateral gastrocnemius worked only in the ascending region of the force-length relationship (Maganaris, 2003), and the tibialis anterior and soleus in

the ascending and plateau region (Maganaris, 2001). Some other studies were interested in the force-length relationship of the muscle producing power during cycling, with the hypothesis that this should be related to cycling performance. Vastus lateralis was found to work in the plateau and descending limb of the force-length relationship, indicating that independent of the cycling effort, this muscle appeared to be used optimally for upright cycling (Austin, Nilwik, & Herzog, 2010; Muraoka, Kawakami, Tachi, & Fukunaga, 2001); however, these results were limited to upright cycling.

It is reasonable to hypothesise that different cycling postures could be related to different behaviours of the human machine, especially in term of performance. Based on these considerations, the purpose of our study was to investigate the non-aerodynamics factors affecting the two different bicycles starting from an experimental approach and theoretical simulations:

i) The 3D displacement of BCoM as a variable involved in the estimation of mechanical power, which is crucial to energy expenditure and the symmetry of its path as potential index measures of motion stability.

ii) The components of the total mechanical work (W_{TOT}) necessary to sustain cycling at various cadences and corresponding external power ($\dot{W}_{EXT}$). From partitioning of internal power ($\dot{W}_{INT}$) and additional external work rate ($\dot{W}_{EXT*}$), it will be possible to understand how each component contributes to the total mechanical work, with consequences on athlete training and bicycle design.

iii) Lower limb muscle-tendon lengths (MTL), which can change in the two different configurations, with the muscles working at different lengths different from their optimal.

Methods

Participants

Four healthy male volunteers (age 28.3 ± 2.6 years; body height 1.77 ± 0.06 m; body mass 66.75 ± 4.11 kg) were recruited. All participants were fit recreational cyclists, who practiced sport (not specifically cycling) 3 times per week (less than 2 hours per week). The University of Milan institutional ethics committee approved all methods and procedures, and participants, fully informed about the aim of the study, gave their written consent prior to the start of testing. Sample size was chosen considering that this work consists of a preliminary comparison between RB and NB and the range of variability in the analysed parameters still remains to be determined. In addition, cycling is a constrained stereotyped movement giving origin to a repeatable kinematics. The consistency of "stereotyped" strides was checked by analysing the BCoM trajectory in local coordinates (on the stationary bikes), both within (intra-subject) and between participants (inter-subject). The variability of strides within each motion capture file was assessed by measuring, point-by-point, the 3D distance between BCoM trajectories of each stride with respect to the others (3D Root Mean Square technique). The average distance for those comparisons represented the consistency of stride trajectories (the smaller the better). The same procedure was applied to all conditions (4 rpm and 2 bicycles) and subjects. The obtained estimates of variability were acceptably low and similar for intra-subject (average distance within participant 0.00199 ± 0.000179 m) and inter-subjects comparisons (average 3D distance among subjects over the four rpm and two bicycles 0.00252 ± 0.000447 m).

Bicycle technical data

The experiments were performed with a "Slyway Hyper" recumbent bicycle (SlyWay®; Slyway Project, Cremona, Italy) and a "Velo Route Tribian 300" upright bicycle (B'Twin®; Decathlon). According to the literature (Reiser, Peterson, & Broker, 2002), the posture of the riders on the bicycles was evaluated in terms of Body Configuration angle (BC) (123 ± 4° in NB and 143 ± 1° in RB), Hip Orientation angle (HO) (75° ± 0° in NB and 0° ± 1° in RB), and Torso angle (TA) (133 ± 4° in NB and 36 ± 2° in RB) (see Figure 1).

Experimental set-up and Protocol

3D kinematic data were obtained with a motion analysis system with 8 infrared cameras (Vicon MX, Oxford Metrics, UK) at a sampling rate of 100 Hz. Thirty-seven reflective markers were positioned on the subject's body landmarks: 35 according to the Plug-In-Gate model (Davis, Ounpuu, Tyburski, & Gage, 1991) which were used to drive a musculoskeletal simulation in OpenSim, and 2 additional markers on the right and left greater trochanter for the computation of BCoM.

After a period of familiarization with the rhythm imposed by a metronome, participants performed one minute of pedalling at 4 different cadences (50-70-90-110 rpm) in randomized order on NB and RB. Moreover, one minute of pedalling against no external resistance (freewheel pedalling) was performed in order to measure the time course of pedal crank angular velocity at self-selected pedalling frequency. Bicycles were stationary, placed on rollers with a constant resistance, and instrumented with an SRM powermeter (Powermeter, SRM, Germany). A digital visual feedback positioned on the bicycle provided the cyclist with the current adopted cadences. At the same cadence $\dot{W}_{EXT}$ was equal in both bicycles, but it increased with pedalling frequency.

Seat to pedal distance (SPD, see Figure 1) was adjusted to 100% of trochanteric leg length, for both NB and RB.

Data Processing

According to previous studies on different locomotion types (Minetti, Ardigò, & Saibene, 1993; Minetti, Pavei, & Biancardi, 2012) 18 of the 37 markers were selected in order to detect 12 body segments. Their fractional mass, centre of mass and the moment of inertia (Winter, 1979) were used to determine the 3D position of the BCoM and the linear and angular speed of segments at each frame. The trajectory of the BCoM has been described with a Lissajous contour, a convoluted loop showing its 3D displacement with respect to the average position. This path described both its kinematical and dynamical features and was obtained by applying the mathematical framework proposed by Minetti et al. (Minetti, Cisotti, & Mian, 2011) based on Fourier analysis. This procedure also allows computation of the Symmetry Indices (*SI*) of the BCoM along the 3 spatial axes, which are expected to be equal to 1 in the case of perfect symmetry between right and left pedalling.

Starting from the 3D position of the BCoM, its associated energies could be evaluated. Potential (*PE*) and Kinetic Energy on antero-posterior (*KEx*), vertical (*KEz*) and medio-lateral (*KEy*) axes were measured with a custom program written in LabView (ver. 8.6 National Instruments) (Minetti, 1998). $\dot{W}_{EXT*}$ was computed as the ratio between the sum of positive changes of the total mechanical energy ($TE=PE+KEx+KEz+KEy$) of BCoM (when the speed of progression is considered 0) during the pedalling cycle and the time of pedal revolution. Notably, because *KEx* depends on the difference between the squares of speed, the contribution of $\dot{W}_{EXT*}$ could

be greater during real cycling on the road (a speed change of 0.1 m/s results in a higher *KEx* if occurring at 5 m/s rather than at 2 (or 0) m/s). $\dot{W}_{INT}$ was calculated as the sum of kinetic linear and angular energies of the segments relative to the BCoM (Cavagna & Kaneko, 1977), while $\dot{W}_{EXT}$ was directly measured from the SRM.

Lower limb MTL were estimated with the musculoskeletal modelling software OpenSim 2.4. (Delp et al., 2007). Marker position data, together with body mass, were used to scale the Gait2392 model through the scaling tool of OpenSim. The model had 23 degrees of freedom and 92 musculo-tendon actuators to represent 76 muscles in the lower extremities and torso. Successively, the inverse kinematics tool was used to compute joint angles of the scaled model that best reproduced the subject's motion. All MTL were computed for both legs and normalized to standing length but, similarly to other studies (Sanderson et al., 2006; Austin et al., 2010), the muscles listed in Table 3 were analysed for the right side of the body only.

Computer physical simulation of pedalling cyclist

In order to verify BCoM trajectory in the sagittal plane, $\dot{W}_{EXT*}$, and $\dot{W}_{INT}$, and successively compare these data with experimental results, a dynamical simulation of a pedalling cyclist was built using Working Model (WM) 2D (Design Simulation, US). The subject was modelled with rectangular segments, with a mass of 51.0, 7.5 and 4.5 kg respectively for head-trunk, thigh (upper leg) and shank (lower leg), connected by frictionless pin joints. The distal portion of the shank was attached to a chain ring where a motor allowed the movement with imposed angular speed corresponding to 50, 70, 90 and 110 rpm. Normal and recumbent postures were reproduced by changing the orientation of the pedalling cyclist (Figure 2). In agreement with previous work

(Minetti, 2011), the chain ring continued to revolve even when the motor was switched off (like in freewheel pedalling), showing a passive endless dynamics that occurred at fluctuating angular speed of the pedals (Figure 3). With the hypothesis that the human body is not perfectly symmetrical and the BCoM profile could be affected by differences in the two lower limbs, we simulated the effect of anatomical asymmetry by shortening one of the two lower legs.

Statistical analysis

To evaluate the effect of different pedalling cadences and bicycles, a two-way ANOVA (bicycle X rpm) for repeated measures with a post-hoc Bonferroni correction was performed on the following parameters: BCoM excursion, symmetry indices (*SIx, SIy, SIz* respectively for antero-posterior, medio-lateral and vertical axis), $\dot{W}_{INT}$ and $\dot{W}_{EXT*}$. With the hypothesis that cadence has no effect on MTL, the behaviour of each analysed muscle was compared for the different bicycles with a paired t-test without taking into account the different rpm. Statistical significance was accepted when $p<0.05$.

Results

The 2D BCoM trajectory in the sagittal plane obtained from WM simulation described an elliptical profile with different major axis inclinations for the two bicycles. Two typical limb configurations named P and λ were identified in the sagittal plane, where the boundary of the major axis of the ellipse described by the BCoM is reached regardless of the position of the subject. The analysis of "freewheel cycling" on NB at self selected pedalling cadence showed similarities with WM simulation. Despite the subjects pedalling at self selected cadence, it showed a fluctuation of pedal crank

angular velocity similar to the WM simulation, and higher speed values were recorded in P limb configurations in both cases (at 10 and 60% of the pedalling cycle in Figure 3). The only difference in the experimental data was related to the presence of two velocity peaks (dashed line in Figure 3) and only one in WM simulation (continuous line).

A similar elliptical profile of BCoM was observed in the real path obtained from experimental session recordings (Figure 4C). 3D examples of the Lissajous contours of the BCoM of a typical participant while pedalling at 90 rpm on NB and RB (Figure 4D and 4E respectively) were also recorded. The 3D BCoM trajectories described different paths for the two bicycles. A greater excursion was observed both for NB and RB in the medio-lateral (y) axis compared to the antero-posterior (x) (+ 56% and 38% respectively on NB and RB) and vertical (z) (+ 22% and 38% respectively on NB and RB). However, the oscillation in forward direction seems to be smaller in NB (6.5 ± 1.2 mm) compared to RB (9.4 ± 2.0 mm), in which narrower oscillation in the vertical axis was observed (NB: 11.6 ± 1.5 mm, RB: 9.4 ± 2.6 mm). Volume was not influenced by pedalling frequency (Table 1).

The right/left symmetry indices along the antero-posterior, medio-lateral and vertical axes (*SIx, SIy, SIz* respectively) reached the highest value in the vertical axis (0.908 ± 0.046) for both bicycles (Figure 5). In the other directions, a different trend for the two pedalling configurations was noticed. While for the NB the lowest symmetry values occurred in the antero-posterior direction, RB reached a minimum in the medio-lateral axis. *SIx* was higher for RB compared to NB, and this difference increased with pedalling frequency ($p<0.05$). Conversely, *SIy* was slightly higher in NB ($p<0.05$).

$\dot{W}_{EXT}$ measured by the SRM for the same cadence can be considered constant during all experimental sessions (38 ± 2, 59 ± 2, 80 ± 5, 105 ± 7 W respectively for 50, 70, 90, 110 rpm). The mechanical internal work rate, or internal power, ranged from 7.90 W ± 0.8 to 65.15 ± 2.99 W for NB and from 7.25 ± 0.82 W to 62.16 ± 9.21 W for RB, increasing as function of the rpm, with the following regression equation:

$$\dot{W}_{INT} = k \cdot m \cdot fr^3$$

where *k* was found to be 0.163 and 0.178 respectively for RB and NB, *m* is the mass of a subject in kg, and *fr* the pedalling frequency in Hz. Data reflected the curve proposed by Minetti in 2001, as indicated in Figure 6A. No significant difference was found between bicycles in $\dot{W}_{INT}$ and values obtained from the WM simulation were the same in upright (NBWM) and recumbent (RBWM) posture (Figure 6A). The additional external mechanical power was always higher in NB compared to RB in both real and simulated pedalling tasks, although significant differences were found between bicycles in real conditions only at specific cadences (Figure 6B). The division of the total mechanical power into its components (internal, external, and additional external) at different pedalling frequencies is reported for both bicycles in Figure 7 and Table 2.

Results from the Opensim simulations are reported in terms of percentage of the standing length (Table 3). The middle point of contraction (the average between maximal and minimal length reached during pedalling cycles) of each MTL was also calculated. For RB, Short Biceps Femoris (+1.3%), Iliacus (+2.6%) and Psoas (+1.9%) were more stretched when compared to NB; Gluteus Maximus (-1.8%) and the three Vasti (-1.8%) were shortened, while other muscles showed no differences.

Discussion

The purpose of our study was to compare NB and RB through the investigation of the non-aerodynamic factors affecting performance on both bicycles (e.g., BCoM trajectories, mechanical work rate and MTL changes).

Our data confirm that the BCoM contour travels, in local coordinates, along a trajectory similar to an ellipse in the sagittal plane (Figure 4C) as anticipated by a simulation (Minetti, 2011), with differences in the major axis inclination between bicycles (more perpendicular to the ground for NB compared to RB; this is reflected by the difference of excursions on *x* and *z* axes). The BCoM moved inside a cube with a side length smaller than 15 mm without significant differences in the two bicycles. Indeed, the excursion of BCoM was greater in the progression axis in RB compared to NB while lower in the vertical one and, consequently, the volume occupied did not differ. In the frontal plane, the BCoM trajectory was in the form of a "U" for NB (Figure 4D) and of an inverted "U" for RB (Figure 4E). In the transverse plane, a figure of "8" was drawn for both bicycles. The BCoM excursion seemed to increase with pedalling frequency, but without significant difference, both for NB and RB. The comparison between the real BCoM paths experimentally obtained and the 2D BCoM trajectories from WM simulation showed differences that can be attributed to the slight discrepancy in the body segments lengths and to the small motion of the 'real' trunk. Looking at Figure 4B, when one of the two limbs in WM simulation was shortened by 1 cm replicating a physiological and common anatomical asymmetry between limbs (Seminati et al., 2013), the BCoM trajectories become similar to the experimental condition (Figure 4C). This supports the hypothesis that anatomical asymmetry may cause dynamical and spatial asymmetry of the BCoM in locomotion with consequences for the motion stability (Gurney, Mermier, Robergs, Gibson, & Rivero, 2001; Seminati

et al., 2013; Biancardi, Fabrica, Polero, Loss, & Minetti, 2011). In this study the highest symmetries were reached in the vertical axis on both bicycles, likely because the saddle limited the movements in this direction. In the antero-posterior axis the RB showed higher symmetry values, compared to NB, and this can be attributed to the backrest that stabilizes the trunk and inhibits its movement in the progression axis. In the medio-lateral axis, symmetry values were always higher for NB and it was not affected by the pedalling frequencies. On both bicycles there are no constraints limiting movements in the frontal plane, and this was more evident in the RB at low rpm likely because each participant was more practiced with cycling on NB. Skilled and trained cyclists could be more symmetrical than the amateur participants who took part in this study. For this reason further analysis could compare experienced riders on RB and NB to investigate which bicycle allows higher dynamical symmetry, and whether training level could have an effect on symmetry.

The position of the BCoM and its displacement also influenced the estimation of mechanical energy expenditure and rider performance. The analysis of the $\dot{W}_{TOT}$ components necessary to sustain the same pedalling task showed that the relationship between cadence and $\dot{W}_{INT}$ on RB was in line with previous results (Minetti et al., 2001). $\dot{W}_{INT}$ was related principally to the pedalling frequency (Figure 6A) with no differences between NB and RB. Internal power has to be considered when riding a bicycle (Francescato et al., 1995), because it is associated to an increment of oxygen consumption (Coast, Cox, & Welch, 1986). However, the metabolic cost could become higher at elevated cadences even without additional mechanical work; an increased rpm implies higher muscle contraction velocity, altering muscle efficiency (Kautz & Neptune, 2002). On the other hand, the relative importance of the 'kinetic' component

of internal work has been questioned, as the WM simulation of pedalling showed that pedal rotation could occur indefinitely with no need for additional power input (Minetti, 2011). This suggests that the measurable (but possibly meaningless) 'kinetic' internal work could be proportional to the non-measurable (likely meaningful) 'viscous' internal work, which could represent the real determinant of the VO2 increment due to high pedalling rate.

In addition, Minetti (2011) suggested a supplementary component of $\dot{W}_{TOT}$, i.e. the $\dot{W}_{EXT*}$ necessary to lift and accelerate the BCoM even during stationary cycling. Both experimentally and in WM physical simulation, $\dot{W}_{EXT*}$ was found to be greater in NB than RB for all cadences (Figure 6B) due to the changed orientation of BCoM profile while pedalling. The $\dot{W}_{EXT*}$ differences between NB and RB were due principally to the vertical excursion of the BCoM on the two bicycles. Changes in potential energy have been observed between bicycles, within the trajectory of the BCoM (on average 4.72 J on NB vs 2.51 J on RB for Working Model simulations and 13.89 J on NB vs 10.84 J on RB for experimental conditions). Conversely, the kinetic energy associated to the BCoM changed with pedalling frequency, but was similar on both bicycles (on average 0.11 J both on NBWM and RBWM and 0.68 J on NB vs. 0.51 J on RB). This contribution potentially increases the total mechanical work and, as a consequence, the metabolic requirements. In absence of a clear theory about the mechanical relevance of $\dot{W}_{EXT*}$, excessive BCoM excursion should be avoided in order to improve cycling locomotion in terms of metabolic cost. This analysis seems to indicate that what was previously assumed to be related just to the W_{INT} (pedalling kinematics) might have some relevance for the computation of the additional external work (BCoM movements, in addition to rolling resistance and air drag). This could

occur in cycling as a result of some energy exchange between limbs through the crank, as previously hypothesized (Kautz & Neptune 2002). Although the energy exchange hypothesis helps to explain the endless revolution of the pedals that occurs in simulations, its role in determining the lateral component of $\dot{W}_{EXT*}$ as measured from 3D kinematics (Table 2), and its metabolic relevance, still remain to be investigated. These uncertainties arise from the fact that, contrary to general belief, the BCoM does not travel parallel to the ground at a constant speed during cycling.

The effect of posture on the rider was investigated, with the hypothesis that one of the two pedalling positions could be more advantageous than the other because of the range of contraction of different muscle-tendon units. Despite the small MTL differences on the two bicycles, it is known that the optimal operative range of the sarcomere is only 5-10% of its maximal length (Cutts, 1988; Rassier, MacIntosh, & Herzog, 1999; Burkholder & Lieber, 2001) and different muscles work in a small portion of the force-length relationship graph. For this reason, even small differences could be important to optimize performance. Since the vastus lateralis muscle works in the plateau and descending limb of the force-length relationship during normal cycling (Austin et al., 2010; Muraoka et al., 2001) and this muscle was shortened on RB in our results, it probably operates nearer its optimal length on RB than NB. Unfortunately, data regarding the force-length relationship during cycling for the other muscles reported in Table 3 are not available in literature and this study cannot conclude whether they work in a portion closer to, or farther from, their optimal length. Although the MTL (the distance between origin and insertion of a muscle) was estimated, this is not enough to simulate the muscle force-length behaviour and force velocity-properties. This analysis could be the starting point for further investigations. Indeed, differently from the MTL estimation that needs only kinematic data (Riley, Franz, Dicharry, &

Kerrigan, 2010), the force across muscle fibres could be investigated with a forward dynamic analysis completed with joint kinematics (Thelen et al., 2005; Zajac, 1989), with a much more complex experimental setup and several assumptions.

Conclusion

This study confirms experimentally the existence of a 3D BCoM movement potentially associated with some additional mechanical external work, previously evaluated only with a computer physical cycling simulation, both for NB and RB. The between-bicycle comparison showed that the BCoM changed its orientation while maintaining a similar pattern in both configurations, with some advantages for the RB: a smaller $\dot{W}_{EXT*}$ and a greater *SIx*. However, although results reported that muscles were working at slightly different operative ranges of their length, the final propulsive effectiveness is difficult to assess, because the differences did not exceed 4% of standing length. From a kinematical perspective, we could speculate that the RB position can be partially (but not completely) considered a 75°-100° backward rotated NB in the sagittal plane, around the mediolateral axis. Indeed, the different body configuration (BC) angle in the two positions causes small but significant changes at iliacus, psoas and thigh muscles. Therefore, we can conclude that only small differences are appreciable between the two bicycles. The principal benefit associated with riding a RB is therefore the aerodynamic factor and the removal of the saddle (Gross et al., 1983), which often causes discomfort to cyclists. The development of mechanisms reducing the energy expenditure related to the $\dot{W}_{EXT*}$ and strategies increasing bicycle stability could be the starting point to further improve the design and performance of these vehicles.

References

Austin, N., Nilwik, R., & Herzog, W. (2010). In vivo operational fascicle lengths of vastuslateralis during sub-maximal and maximal cycling. *Journal of Biomechanics*, 43, 2394–2399.

Biancardi, C. M., Fabrica, C. G., Polero, P., Loss, J. F., & Minetti, A. E. (2011). Biomechanics of octopedal locomotion: kinematic and kinetic analysis of the spider Grammostolamollicoma. *The Journal of Experimental Biology*, *214*(20), 3433-3442.

Burkholder T. J., & Lieber R. L. (2001). Sarcomere length operating range of vertebrate muscles during movement. *The Journal of Experimental Biology,* 204, 1529–1536.

Cavagna, G. A., & Kaneko, M. (1977). Mechanical work and efficiency in level walking and running. *The Journal of Physiology*, *268*(2), 467-481.

Coast, J. R., Cox, R. H., & Welch, H. G. (1986). Optimal pedalling rate in prolonged bouts of cycle ergometry. *Medicine and Science in Sports and Exercise*, *18*(2), 225-230.

Cutts A. (1988). The range of sarcomere lengths in the muscles of the human lower limb. *Journal of Anatomy*, 160, 79-88.

Davis III, R. B., Ounpuu, S., Tyburski, D., & Gage, J. R. (1991). A gait analysis data collection and reduction technique. *Human Movement Science*, *10*(5), 575-587.

Delp, S. L., Anderson, F. C., Arnold, A. S., Loan, P., Habib, A., John, C. T., & Thelen, D. G. (2007). OpenSim: open-source software to create and analyze dynamic simulations of movement. *IEEE Transactions on Biomedical Engineering*, *54*(11), 1940-1950.

Faria, E. W., Parker, D. L., & Faria, I. E. (2005). The science of cycling: factors affecting performance–part 2. *Sports Medicine*, *35*(4), 313-337.

Fenn, W. O. (1930). Frictional and kinetic factors in the work of sprint running. *American Journal of Physiology--Legacy Content*, *92*(3), 583-611.

Francescato, M. P., Girardis, M., & Di Prampero, P. E. (1995). Oxygen cost of internal work during cycling. *European Journal of Applied Physiology and Occupational Physiology*, *72*(1-2), 51-57.

Gross, A. C., Kyle, C. R., & Malewicki, D. J. (1983). The aerodynamics of human-powered land vehicles. *Scientific American*, 249(6), 142-152.

Gurney, B., Mermier, C., Robergs, R., Gibson, A., & Rivero, D. (2001). Effects of limb-length discrepancy on gait economy and lower-extremity muscle activity in older adults. *The Journal of Bone & Joint Surgery*, *83*(6), 907-915.

Kautz, S. A., & Neptune, R. R. (2002). Biomechanical determinants of pedaling energetics: internal and external work are not independent. *Exercise and sport sciences reviews*, *30*(4), 159-165.

Maganaris, C. N. (2001). Force–length characteristics of in vivo human skeletal muscle. *Acta Physiologica Scandinavica*, *172*(4), 279-285.

Maganaris, C. N. (2003). Force-length characteristics of the in vivo human gastrocnemius muscle. *Clinical Anatomy*, *16*(3), 215-223.

Minetti, A. E., Ardigo, L. P., & Saibene, F. (1993). Mechanical determinants of gradient walking energetics in man. *The Journal of Physiology*, *472*(1), 725-735.

Minetti, A. E. (1998). A model equation for the prediction of mechanical internal work of terrestrial locomotion. *Journal of Biomechanics*, *31*(5), 463-468.

Minetti, A. E. (2004). Passive tools for enhancing muscle-driven motion and locomotion. *Journal of Experimental biology*, 1265-1272.

Minetti, A. E. (2011). Bioenergetics and biomechanics of cycling: the role of 'internal work'. *European Journal of Applied Physiology*, *111*(3), 323-329.

Minetti, A. E., Cisotti, C., & Mian, O. S. (2011). The mathematical description of the body centre of mass 3D path in human and animal locomotion.*Journal of Biomechanics*, *44*(8), 1471-1477.

Minetti, A. E., Pavei, G., & Biancardi, C. M. (2012). The energetics and mechanics of level and gradient skipping: Preliminary results for a potential gait of choice in low gravity environments. *Planetary and Space Science*, *74*(1), 142-145.

Minetti, A. E., Pinkerton, J., & Zamparo, P. (2001). From bipedalism to bicyclism: evolution in energetics and biomechanics of historic bicycles. *Proceedings of the Royal Society of London. Series B: Biological Sciences*, *268*(1474), 1351-1360.

Muraoka, T., Kawakami, Y., Tachi, M., & Fukunaga, T. (2001). Muscle fiber and tendon length changes in the human vastuslateralis during slow pedaling. *Journal of Applied Physiology*, *91*(5), 2035-2040.

di Prampero, P. F., Mognoni, P., Saibene, F. (1979) Internal power in cycling. Experientia [Abstr] 351925.

Rassier D. E., MacIntosh B. R., & Herzog W. (1999). Length dependence of active force production in skeletal muscle. *Journal of Applied Physiology,* 86:1445-1457.

Reiser, R. F. & Peterson, M. L., (1998). Lower-extremity power output in recumbent cycling: a literature review. *Human Power*, volume 13, number 3, Summer/Fall.

Reiser, R. F., Peterson, M. L., Broker, J. P. (2002). Influence of hip orientation on wingate power output and cycling technique. *Journal of Strength and Conditioning Research* 16:556–560.

Riley, P. O., Franz, J., Dicharry, J., & Kerrigan, D. C. (2010). Changes in hip joint muscle–tendon lengths with mode of locomotion.*Gait & Posture*, *31*(2), 279-283.

Sanderson, D. J., Martin, P. E., Honeyman, G., & Keefer, J. (2006). Gastrocnemius and soleus muscle length, velocity, and EMG responses to changes in pedalling cadence. *Journal of Electromyography and Kinesiology, 16*(6), 642-649.

Seminati, E., Nardello, F., Zamparo, P., Ardigò, L. P., Faccioli, N., & Minetti, A. E. (2013). Anatomically Asymmetrical Runners Move More Asymmetrically at the Same Metabolic Cost. *PloS one*, *8*(9), e74134.

Thelen, D. G., Chumanov, E. S., Hoerth, D. M., Best, T. M., Swanson, S. C., Li, L., & Heiderscheit, B. C. (2005). Hamstring muscle kinematics during treadmill sprinting. *Medicine and Science in Sports and Exerc*ise,*37*(1), 108-114.

Too, D. (1990). Biomechanics of cycling and factors affecting performance. *Sports Medicine*, *10*(5), 286-302.

Winter, D. A. (1979). A new definition of mechanical work done in human movement. *Journal of Applied Physiology*, *46*(1), 79-83.

Zajac, F. E. (1988). Muscle and tendon: properties, models, scaling, and application to biomechanics and motor control. *Critical Reviews in Biomedical Engineering*, *17*(4), 359-411.

Table 1. BCoM excursion (in mm) in three axes and BCoM volume (in mm^3) on both bicycles ± *SD*.

NB				
rpm	x (mm)	y (mm)	z (mm)	Vol (mm^3)
50	8.0 ± 2.9	14.0 ± 3.2	10.0 ± 0.6*	1177.2 ± 694.7
70	6.8 ± 2.6*	15.0 ± 3.9	11.0 ± 1.1*	1144.8 ± 559.4
90	5.2 ± 1.3*	15.3 ± 3.8	12.1 ± 1.4	996.9 ± 482.5
110	5.9 ± 0.7	14.8 ± 6.4	13.4 ± 2.7	1221.2 ± 826.0
M	6.5 ± 1.2	14.8 ± 0.5	11.6 ± 1.5	1135.0 ± 591.3
RB				
rpm	x (mm)	y (mm)	z (mm)	Vol (mm^3)
50	10.2 ± 1.7	10.7 ± 7.1	6.9 ± 1.9*	830.5 ± 782.7
70	11.6 ± 1.2*	15.6 ± 5.4	7.8 ± 1.8*	1511.9 ± 949.9
90	9.0 ± 1.5*	17.5 ± 2.8	10.3 ± 2.4	1651.3 ± 653.5
110	6.8 ± 2.5	16.8 ± 4.0	12.6 ± 2.8	1533.8 ± 912.8
M	9.4 ± 2.0	15.1 ± 3.1	9.4 ± 2.6	1381.9 ± 816.9

* indicates significant difference between bicycles ($p < 0.05$).

Table 2: Values of external ($\dot{W}_{EXT}$), additional external ($\dot{W}_{EXT*}$) and internal ($\dot{W}_{INT}$) power for the two bikes in the 4 experimental sessions expressed in Watt. Significant differences are reported in Figure 6.

	NB			RB		
rpm	$\dot{W}_{EXT}$	$\dot{W}_{EXT*}$	$\dot{W}_{INT}$	$\dot{W}_{EXT}$	$\dot{W}_{EXT*}$	$\dot{W}_{INT}$
50	36.7 ± 1.7	11.0 ± 1.0	7.9 ± 0.8	38.5 ± 1.5	6.4 ± 1.3	7.3 ± 0.5
70	59.7 ± 2.1	16.2 ± 2.0	19.6 ± 2.3	57.4 ± 2.5	10.7 ± 3.0	17.9 ± 1.0
90	81.3 ± 4.2	22.5 ± 3.8	39.2 ± 1.6	79.0 ± 5.6	19.0 ± 5.1	37.3 ± 1.6
110	109.1 ± 8.4	31.4 ± 6.6	65.2 ± 3.0	103.6 ± 7.2	28.4 ± 4.5	62.2 ± 9.2

Table 3. Maximal and Minimal MTL (% of resting length) reached by different Muscle Tendon Unit (MTU) in RB and NB; the difference between maximal and minimal MTL reached is the range of contraction of the MTU and is reported as 'excursion'.

	NB			RB		
	Max	Min	Excursion	Max	Min	Excursion
BiFemSh	91.9 ± 2.5*	76.7 ± 0.7*	15.2 ± 2.1*	94.2 ± 1.8	77.1 ± 0.6	17.1 ± 2.0
Gmax	129.2 ± 1.2	116.9 ± 2.3*	12.4 ± 2.0*	128.2 ± 1.7	114.3 ± 2.4	13.9 ±1.1
Iliac	85.9 ± 3.0*	71.1 ± 1.1*	14.7 ± 1.6*	88.8 ± 2.2	73.4 ± 2.1	15.4 ±1.1
Psoas	88.9 ± 2.2*	77.9 ± 0.9*	11.0 ± 1.2*	91.1 ± 1.7	79.7 ± 1.8	11.5 ± 0.8
Vas Int	137.2 ± 2.0*	114.6 ± 3.4*	22.6 ± 0.8*	136.7 ± 1.5	111.5 ± 1.9	25.2 ± 0.7
Vas Lat	133.0 ± 1.8*	112.8 ± 3.0*	20.2 ± 1.2*	132.5 ± 1.3	110.2 ± 1.6	22.3 ± 1.1
Vas Med	138.2 ± 2.1*	114.5 ± 3.3*	23.7 ± 3.5*	137.6 ± 1.6	111.5 ± 1.9	26.1 ± 2.2

Notes: BiFemSh, *Short Biceps Femoris;* Gmax, *Gluteus Maximus*; Iliac, *Iliacus*; Vas Int, *VastusIntermedius*; Vas Lat, *VastusLateralis;* Vas Med, *VastusMedialis*. * indicates significant difference between bicycles ($p < 0.05$).

Figure Captions:

Figure 1: A) Geometrical variables describing the position of the riders on a bicycle (adapted from Reiser & Peterson, 1998): Body Configuration Angle (BC), the angle with origin at the hip joint, formed by the trunk and the segment connecting the hip joint and the crank; Hip Orientation (HO), the angle of hip joint centre to bottom bracket relative to horizontal; Torso Angle (TA), the angle between hip-shoulder segment and the horizontal line passing through the hip joint; Seat to pedal distance (SPD). B) RB dimensions: front wheel size: 0.508 m; rear wheel size: 0.660 m; seat angle (α): 30°; head tube angle (β): 72°, wheel base (a): 1.230 m; medium bottom bracket (b): 0.585 m; seat height (c) 0.370 m. C) NB dimensions: wheels size 0.620 m, seat tube angle (α): 75°, head tube angle (β): 68°; wheel base (a) 1.420 m, medium bottom bracket (b): 0.300 m; seat height (c): depending on the trochanteric leg length of the subjects.

Figure 2. Working Model Simulation (WM) of pedalling cyclist on NB with limbs in P configuration and on RB with limbs in λ configuration. Clockwise from upper left, the software output windows show instant values of variables related to: the position of the BCoM; the energies associated to the BCoM and the crank; the velocity of BCoM, the velocity of each segment respect to the BCoM velocity; the kinetic energy associated to each segment; the power needed to the motor to rotate the system; the angular velocity of the crank.

Figure 3: Analysis of "freewheel cycling" (angular speed versus pedalling cycle) on NB at self selected pedalling cadence (within the sagittal plane, with frictionless pin joints, but resulting in fluctuating angular speed). In the fluctuation of pedal crank angular velocity, higher speed values were recorded in P limbs configuration both in experimental sessions (dashed line) and in WM simulations (black line).

Figure 4. BCoM trajectories in the sagittal plane from Working Model symmetrical (A) and asymmetrical (B) simulation (one of the two tibia segments was shortened by 15 mm). The experimental contour in the same plane is also reported for a typical subject (C). Boxes D and E represent the 3D BCoM trajectories of the same subject on the NB (thick black line) and RB (thick grey line). Projections of the BCoM on the different planes (thin lines) are shown on the walls of the cube (side length 20 mm). The black arrow indicates the progression axis.

Figure 5. *SIx* (A), *SIy* (B) and *SIz* (C) at different rpm. Numbers 1, 2, 3, 4 represent significant differences between 50, 70, 90, 110 rpm respectively. * indicates difference between bicycles ($p < 0.05$).

Figure 6. Mechanical internal (A) and additional external (B) power as function of rpm in both real (NB and RB) and simulated (NB WM, RB WM) pedalling task. Numbers 1, 2, 3, 4 indicate significant differences between 50, 70, 90, 110 rpm respectively. * indicates significant difference between bicycles ($p < 0.05$). Dashed line superimposed in panel A shows the polynomial curve proposed by Minetti in 2001.

Figure 7: Mechanical power partitioning (% of the $\dot{W}_{TOT}$) for each pedalling cadence in normal (NB) and recumbent (RB) bicycle.

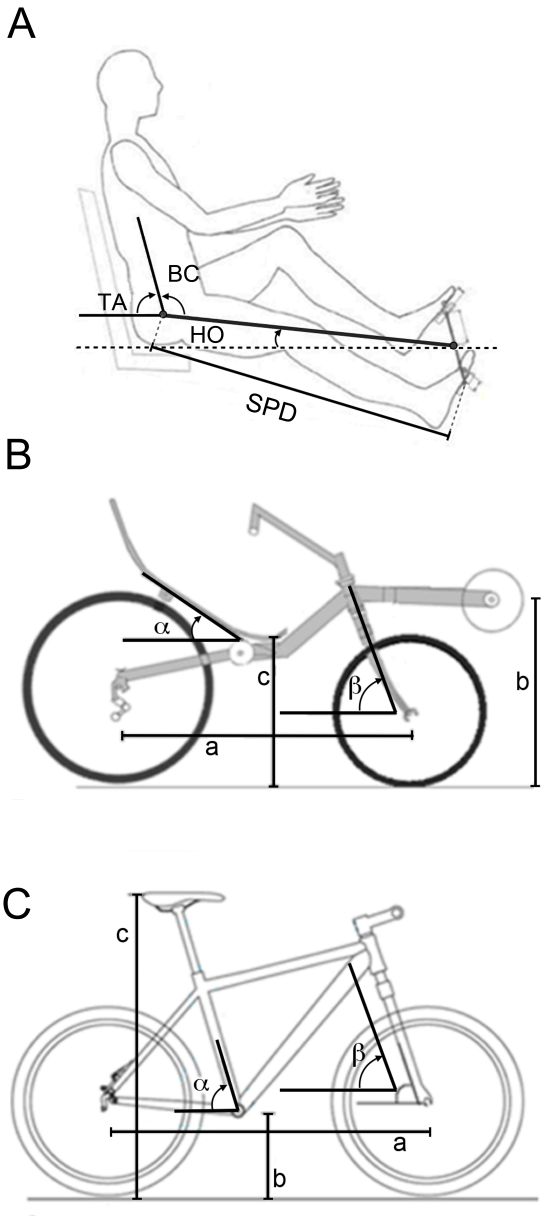

Figure 1

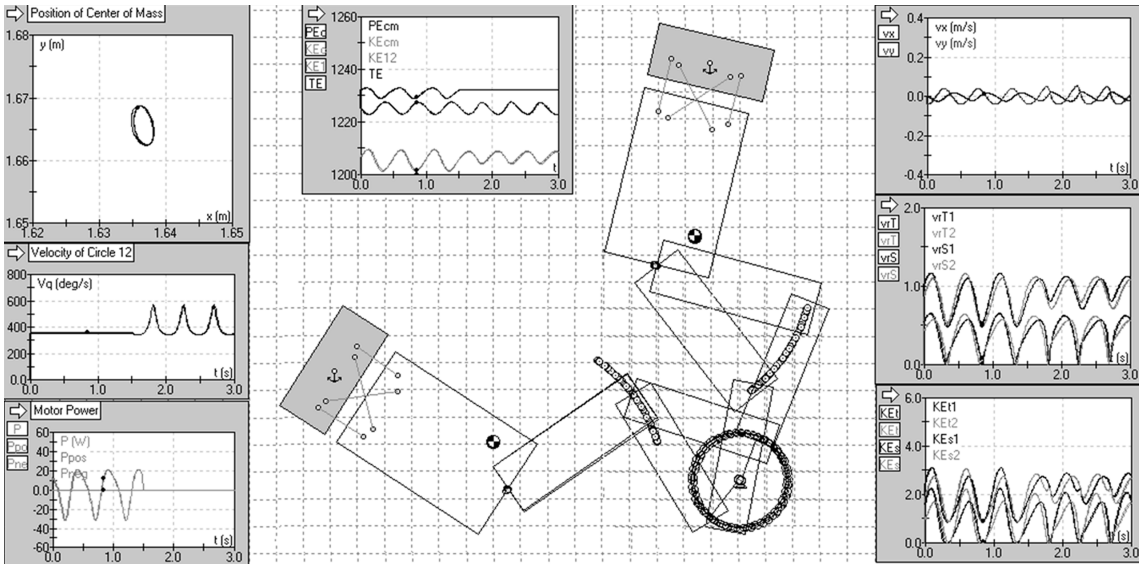
Position of Center of Mass
y (m)
x (m)
Velocity of Circle 12
Vq (deg/s)
t (s)
Motor Power
P (W)
Ppos
Pneg
PEcm
KEcm
KE12
TE
vx (m/s)
vy (m/s)
vrT1
vrT2
vrS1
vrS2
KEt1
KEt2
KEs1
KEs2

Figure 2

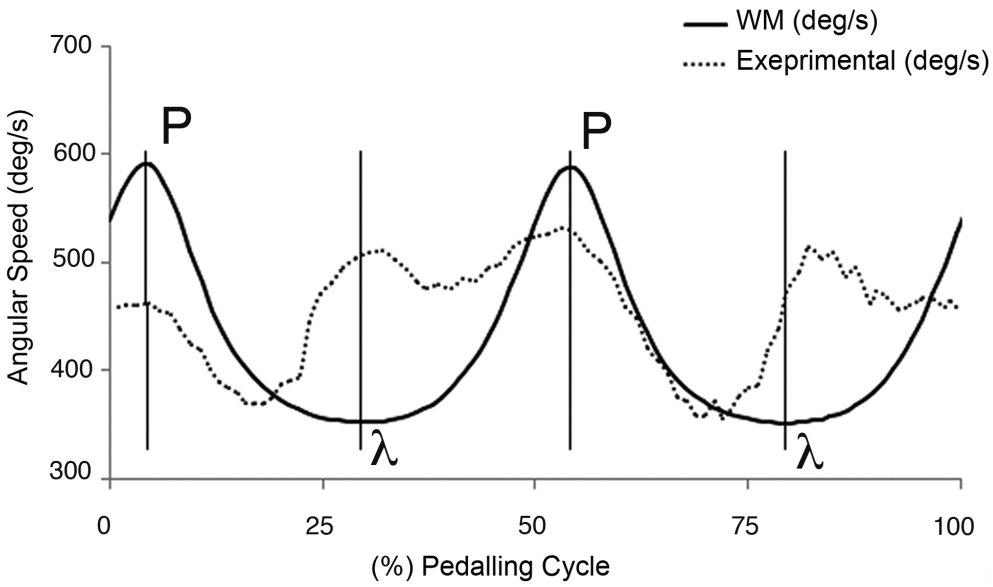
WM (deg/s)
Exeprimental (deg/s)
Angular Speed (deg/s)
700
600
500
400
300
P
P
λ
λ
0
25
50
75
100
(%) Pedalling Cycle

Figure 3

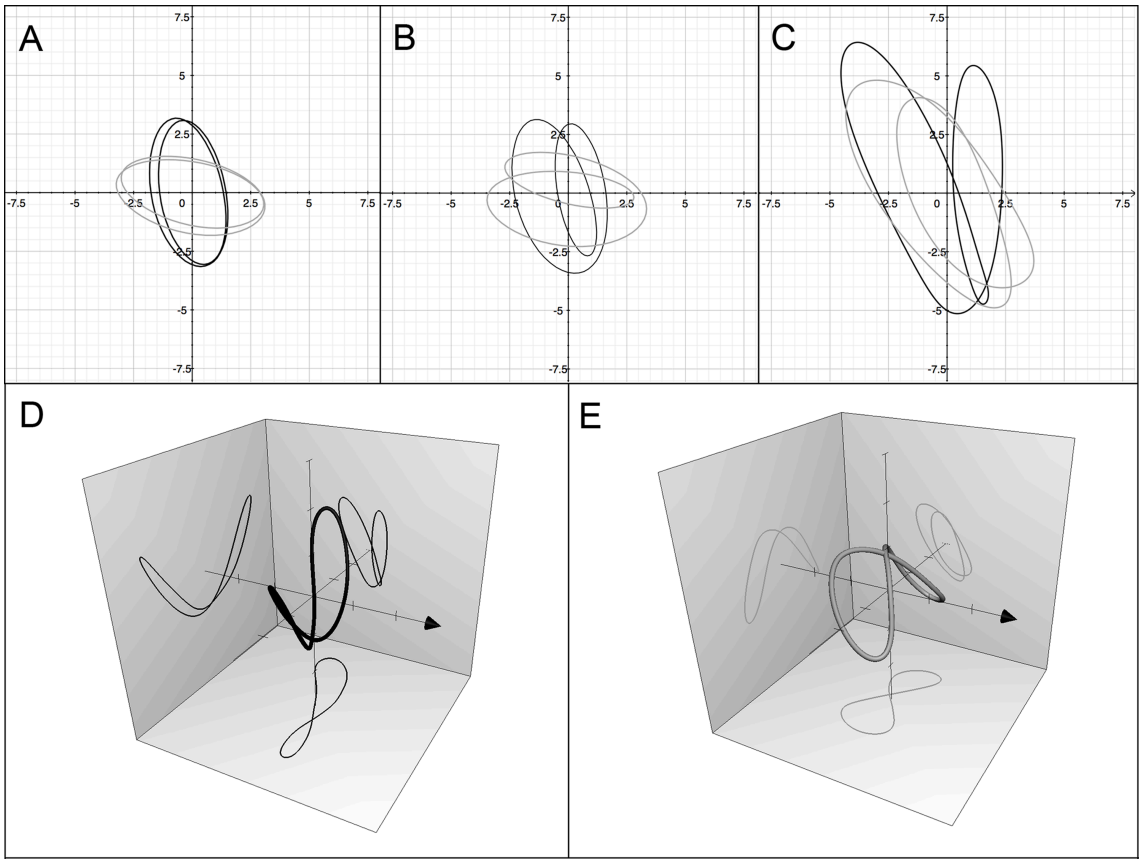

Figure 4

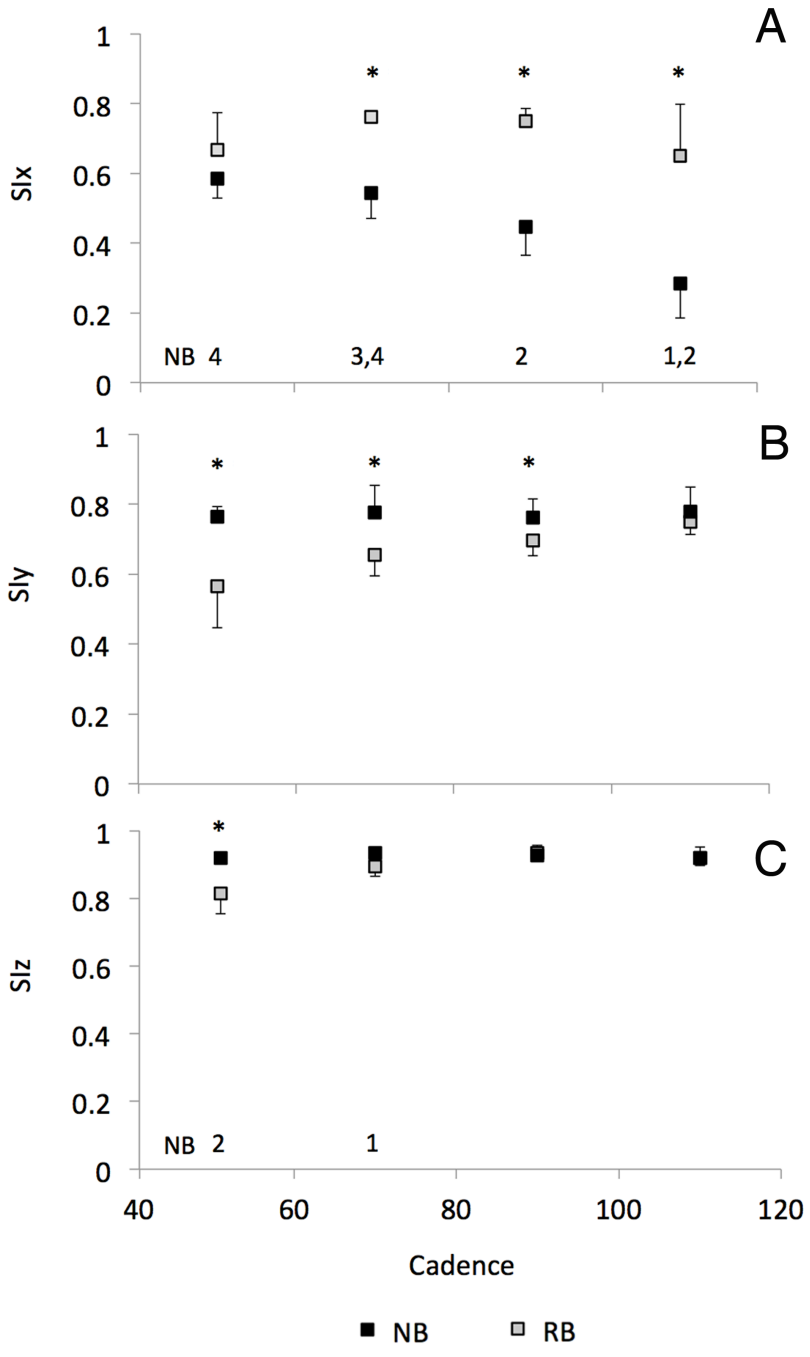
A
B
C
Slx
Sly
Slz
1
0.8
0.6
0.4
0.2
0
*
NB 4
3,4
2
1,2
NB 2
1
40
60
80
100
120
Cadence
NB
RB

Figure 5

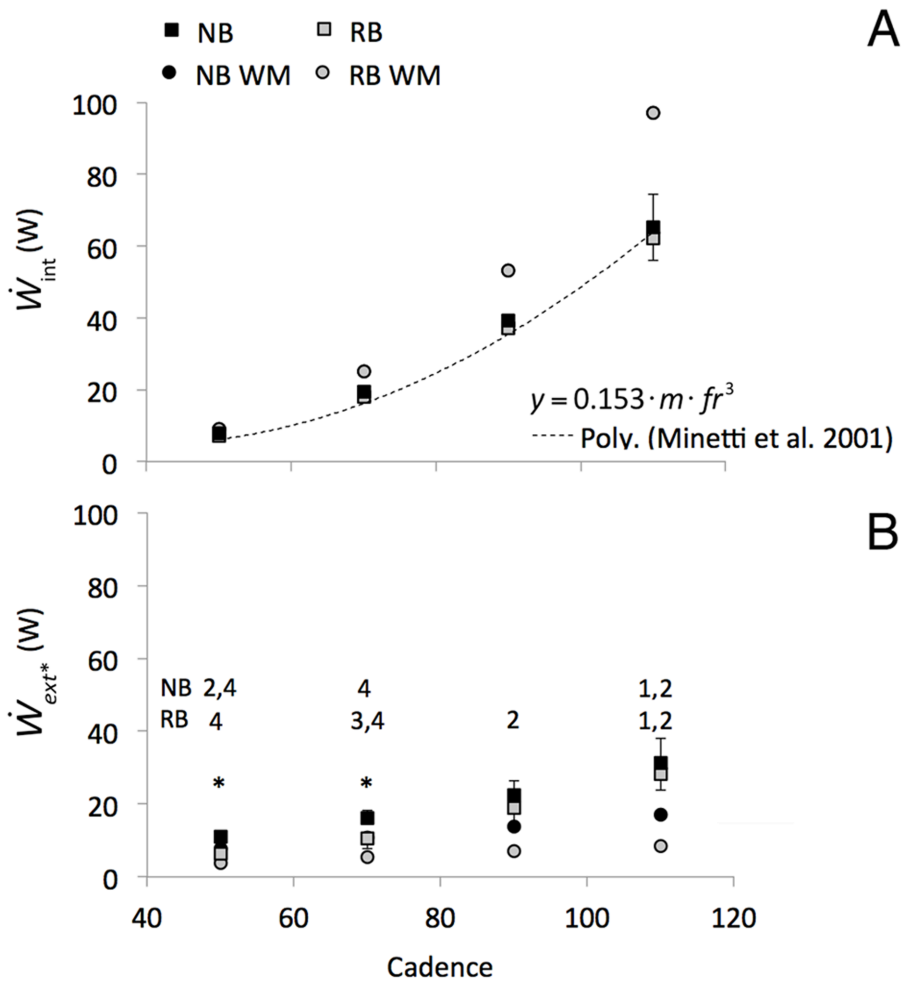
A
NB
RB
NB WM
RB WM
100
80
60
40
20
0
$\dot{W}_{int}$ (W)
$y = 0.153 \cdot m \cdot fr^3$
Poly. (Minetti et al. 2001)
B
100
80
60
40
20
0
$\dot{W}_{ext*}$ (W)
NB 2,4
4
1,2
RB 4
3,4
2
1,2
*
*
40
60
80
100
120
Cadence

Figure 6

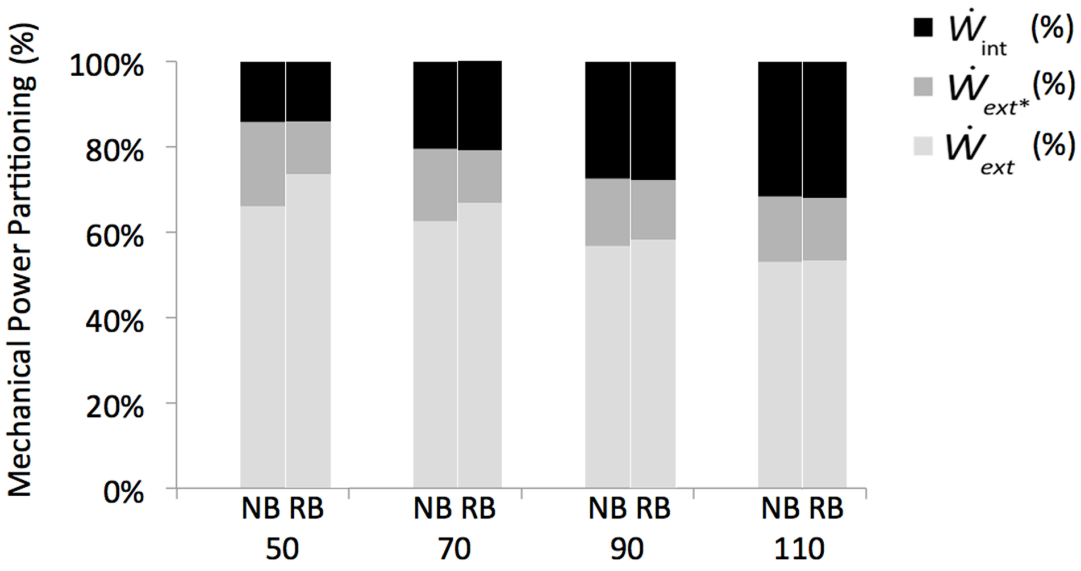
Mechanical Power Partitioning (%)
100%
80%
60%
40%
20%
0%
NB RB 50
NB RB 70
NB RB 90
NB RB 110
$\dot{W}_{int}$ (%)
$\dot{W}_{ext*}$ (%)
$\dot{W}_{ext}$ (%)

Figure 7